

SHUTTLE FLIGHT PRESSURE INSTRUMENTATION:

EXPERIENCE AND LESSONS FOR THE FUTURE

P. M. Siemers III and P. F. Bradley
NASA Langley Research Center
Hampton, Virginia

H. Wolf and P. F. Flanagan
Analytical Mechanics Associates, Incorporated
Hampton, Virginia

K. J. Weilmuenster and F. A. Kern
NASA Langley Research Center
Hampton, Virginia

SUMMARY

Flight data obtained from the Space Transportation System orbiter entries are processed and analyzed to assess the accuracy and performance of the Development Flight Instrumentation (DFI) pressure measurement system. Selected pressure measurements are compared with available wind tunnel and computational data and are further used to perform air data analyses using the Shuttle Entry Air Data System (SEADS) computation technique. The results are compared to air data from other sources. These comparisons isolate and demonstrate the effects of the various limitations of the DFI pressure measurement system. The effects of these limitations on orbiter performance analyses are addressed, and instrumentation modifications are recommended to improve the accuracy of similar flight data systems in the future.

INTRODUCTION

During the first five flights of the Space Transportation System (STS), the orbiter (OV-102) was instrumented to provide the flight data required to evaluate and interpret its performance and thereby verify the vehicle's flight worthiness and mission capability. This instrumentation system, designated Development Flight Instrumentation (DFI), included approximately 4500 measurements of which 200 were surface-pressure measurements intended to assist in the refinement of aerodynamic loads and performance characteristics predictions. It is the primary purpose of this study to evaluate the performance of this DFI pressure measurement system. This evaluation is based on a comparison of flight data obtained from the forward fuselage DFI with wind tunnel and computational data as well as results obtained from postflight analyses incorporating other entry flight data relative to vehicle attitude and state.

The basis for much of the evaluation and recommendations of this study is the experience gained in the development of the Shuttle Entry Air Data System (SEADS) (ref. 1). The SEADS is a new concept in air data systems and consists of an array of flush orifices installed in the nose and forward fuselage of the orbiter. The SEADS will provide research quality air data from Mach 30 to touchdown. The transducers for the SEADS are identical to similarly ranged

DFI transducers and have been rigorously calibrated to provide pressure data to a greater accuracy than available from the DFI. The design of the SEADS and the calibration of the transducers provided generic data applicable to the DFI transducers and pressure data system in general.

In addition, the DFI data have provided the opportunity to verify (in a restricted manner because of the lack of nose cap orifices) the SEADS pressure model incorporated in the data-reduction algorithm. The available data near the nose have been used to predict angle of attack and free-stream dynamic pressure. The results of this SEADS/DFI analysis are compared to other sources of such air data.

This evaluation of the DFI has resulted in a number of recommendations which would enhance the accuracy and usefulness of future flight data systems.

DATA AVAILABILITY

The wind tunnel data were obtained in various ground research facilities using different models. The wind tunnel data range spans the reentry Mach number range from hypersonic ($M = 10.0$) to subsonic ($M = 0.25$) for three different forward fuselage models (0.02 - scale, 0.04 - scale, and 0.10 - scale) (ref. 2). The wind tunnel models were instrumented to duplicate locations of selected orbiter surface DFI pressures as shown in figures 1-3. The computational data were obtained from a solution of the three-dimensional Euler equations about a modified orbiter geometry using the HALIS (ref. 3) computer code for the continuum flow regime at hypersonic Mach numbers. The computational data were also selected to match flight conditions and locations corresponding to these selected DFI pressure sensors. The flight data used in this study are limited to the orifices located in the forward fuselage region because of the limitation of the wind tunnel and computational data (figs. 1-3). Although flight data were measured by the DFI sensors during the orbiter's first five flights, during STS-1 and STS-4 the DFI recorder malfunctioned, thereby restricting the data to those obtained from telemetry after blackout. This limited data to Mach numbers of 13 and below. In addition, due to a power constraint, only a restricted amount of pressure data was available from STS-2. A complete set of data was, however, obtained during STS-3 and -5, which allowed an analysis of the pressure data as well as behavior of the data system. Where comparisons could be performed, pressure data from all flights displayed a high degree of consistency.

DFI FLIGHT DATA ASSESSMENT

As noted in references 2, 4, 5, and 6, several shortcomings in the DFI pressure measurement and data system have been identified that could have a significant effect on the interpretation and application of the flight data. These potential error sources are:

1. Tile Steps and Gaps
2. Port Leakage

3. Transducer Calibration
4. Data System
5. Measurement Location and Range

These error sources have been evaluated and are discussed to quantify DFI pressure uncertainty. This study has resulted in recommendations which could, if incorporated into the DFI or other flight data systems, greatly enhance the accuracy and applicability of the data.

Tile Steps and Gaps

The DFI pressure orifices are generally located near the center of the thermal protection system tile. The orifice penetrates the tile, its bonding material, and the orbiter's aluminum skin (ref. 7). Each instrumented tile is surrounded by other tiles which are separated from one another by a thermal expansion gap. In addition, due to the flexibility of the TPS tile system, steps exist between adjacent tiles. Attempts to quantify the effects of steps and gaps were not entirely successful because of their unpredictability and sensitivity to the thermal environment. Based on the analyses which have been done, the error induced by steps and gaps is below the resolution of the DFI system.

Port Leakage

Port leaks generally occur in the joint at the strain isolation pad (SIP) between the TPS tile and the aluminum skin. These leaks are generally caused when tiles are pull-tested for bond strength and the seal is damaged. Leaks are categorized by the loss of a gas in cm^3/min . Standards for the orifice installation specify a leak rate of over $80 \text{ cm}^3/\text{min}$ to be unacceptable. A comparison of data obtained during STS-2 for two transducers located symmetrically on either side of the fuselage is shown in figure 4. One of the orifices (V07P9115) was leaking in excess of $200 \text{ cm}^3/\text{min}$, while the other (V07P9114) was leaking less than $20 \text{ cm}^3/\text{min}$ in tests completed prior to the flight. In spite of the leak rate difference, the data from the two transducers are in close agreement. Further evidence that tile leakage is a minor factor in measurement accuracy is shown in figure 5 for the port V07P9871. During STS-1, this orifice was covered by a blank tile, but when the flight data are compared to ground-based data as shown in figure 5, the agreement is no better or worse than any other comparisons.

Subsequent to flight 1, the tile at port V07P9871 was replaced with a properly drilled tile. A comparison of the residuals on a common data arc obtained from STS-1 and STS-3, respectively, was made. While certain differences appear, their magnitude is small and well within the error band derived from other pressure measurements.

Additionally, tests conducted at Rockwell International confirmed that the absence of a pressure port tube through the tile introduced a pressure differential of less than 0.3 psf across the tile. This differential is below the resolution of the DFI data system.

It is concluded that the porosity of the orbiter TPS (gaps) allows bleeding of surface pressure to the sensor, and even if the orifice leaks, the effects on the final data are insignificant given the uncertainties in the existing DFI system.

Transducer Calibration

It is the authors' experience that careful calibration of pressure transducers is essential to maximize measurement capability and to obtain accurate, high-resolution flight data. Although the DFI transducers were calibrated individually and their sensitivity determined for three different temperatures, the calibration data for transducers of similar range were averaged, and a universal calibration curve was established. While such a procedure does not use the full capability of the transducers, it is consistent with the 8-bit data system used in the DFI. In contrast, the SEADS calibration program was designed to take advantage of the full capability of the transducers and account for the environmental conditions of temperature, random vibration, acceleration, and mechanical shock. The results of this calibration showed that the performance characteristics were different enough from transducer to transducer to require detailed individual transducer performance characterization.

Forty-nine pressure transducers, identical except for range to existing DFI transducers, were calibrated at the Langley Research Center in support of SEADS. Of these 49 transducers, seven failed or failed to meet specifications and were, therefore, rejected and not included in this study. Analysis of the calibration data from the 42 acceptable transducers clearly demonstrates the need for detailed performance characterization. Although the transducers met procurement specifications, performance differences within tolerance limits are significant. The output of the transducers at a constant temperature and essentially zero pressure (0.001 psia) bias had a distribution (fig. 6) ranging from -2 to +3.5 percent of full scale. The sensitivity distribution for a constant temperature (fig. 7) has a range of -1.5 to +1.25 percent of the average sensitivity for the sample. These data establish the requirement for individual characterization of each transducer included in the system, as well as a requirement on the data system to handle negative voltages. Individual transducer response characteristics, although highly repeatable, are not linear. As a result, simple linear transfer function modeling cannot be used in the analysis of flight data without introducing a significant loss of measurement accuracy.

Linear and second-order least-squares analyses were used to assess transducer nonlinearity and hysteresis at a constant temperature. The distribution of the data (fig. 8) indicates a variation from 0 to 0.5 percent of full scale with approximately 75 percent of this variation due to nonlinearity alone. Repeatability of these data was better than 0.02 percent of full scale, demonstrating that a higher order transfer function will significantly improve pressure measurement accuracy.

Temperature affects both the sensitivity and the zero-pressure output (bias) of the transducers. While the SEADS transducers were calibrated at five temperatures between -79°C and 113°C, figure 9 shows the distribution in the thermal zero-pressure coefficient considering only the end and midpoint

temperatures as was done for the DFI transducers. The coefficient is shown to vary from nearly 0 to 0.05 percent full scale per degree centigrade. In addition, figures 10 and 11 show that while transducer sensitivity is only slightly affected by temperature (0 to 0.011 percent per degree centigrade), the zero-pressure (bias) dependence on temperature is not only nonlinear but also significantly different in character for each transducer. These results substantiate the need for a thorough temperature calibration.

On the basis of these calibration results, it is concluded that the error in the DFI transducers could be as large as 5.0 percent of full scale. To reduce this error and obtain the maximum accuracy (0.1 percent of full scale), it is necessary to obtain in-flight measurements of transducer temperature and zero-pressure bias as well as the accomplishment of a thorough calibration of each transducer and the use of the individual calibration curves corrected for temperature in data reduction.

Analysis of the random vibration test data over a 20- to 2000-hertz range at 22.6 g rms level, performed primarily to insure transducer survivability, resulted in an output noise level of 10 millivolts. Detailed calibration pre- and postshock and thermal cycle should be obtained to characterize flight-to-flight repeatability. (The majority of the transducer failures occurred during the random vibration and shock calibration tests thereby demonstrating the importance of such tests.) The static acceleration tests at 2 g and 5 g for a 5-minute duration showed an output change of approximately 0.010 millivolts. To avoid this error source, transverse mounting of transducers is best although not critical.

Measurements of the transducer output noise level under zero-pressure load indicated an rms noise level of 5 to 10 millivolts generated by the transducer's 20-KHz carrier frequency. Although the noise is indistinguishable within the resolution of the DFI data system, any improvement in resolution would dictate the need for output filters in the system to minimize the effects of this high-frequency noise.

Five transducers were recalibrated after a period of approximately 2 years. Four of the transducers changed sensitivity less than 0.1 percent. The zero-pressure output showed changes between -0.6 percent to +0.5 percent of full scale. In general, the nonlinearity and hysteresis changed less than 0.1 percent of full scale. These data illustrate the stability of these transducers over long periods of time.

Data System

Data rate and resolution are critical to the accurate interpretation of data such as that obtained during the flight of the STS. Data resolution is dependent on the ability of the measurement sensor to detect small changes in the measured value and on the data system's capability to process these data at a comparable resolution.

The DFI data system digitizes the analog output of the transducers. The nominal output range is 0 to 5 volts, whereas both calibration and flight data show that negative voltages occur at 0 or low pressures. Such negative biases are, therefore, not read, and their omission compromises the accuracy of

the data. An 8-bit pulse-code modulator (PCM) is used, and the data are recorded at a rate of 1 sample per second. The resulting resolution of the DFI pressure data is approximately 11.25 psf for the 0-20 psia transducers, 8.44 psf for the 0-15 psia transducers, 0.586 psf for the 0-150 psf transducers, and 0.293 psf for the 0-75 psf transducers. Studies^{4,6} have shown that the DFI data rate and resolution introduce uncertainties into the flight data restricting the ability to verify the performance of the flight system through flight and ground-based data correlations. To resolve such shortcomings, a more thorough analysis of the problem to be solved is mandatory when specifying system resolution and response. The orbiter experiment program (OEX), designed to provide highly accurate, research quality data, uses a 12-bit PCM system and data rates between 2 and 150 samples per second depending on the data type.

The incorporation of high resolution into a data system complicates the overall design because of the system's new sensitivity to electromagnetic interference (EMI) and electronic noise. EMI effects must be minimized by using shielded components, particularly shielded cable, as in the Forward Fuselage Support System for OEX. In a typical pressure system, the transducer is a source of noise; therefore, the transducer design must consider the data resolution requirement. The inclusion of integrated filter circuits in the transducer is desirable, but as in the case of the SEADS transducers, these filter circuit requirements were not defined prior to manufacture. Circuits designed based on component tests were incorporated into the data system's PCM slave. In addition, the increased system resolution results in an increased sensitivity within the data system to supply voltage and temperature, both of which must then be monitored for postflight data correction. Finally, in general, the data system should retain a flexibility to be modified as a result of end-to-end system level tests.

Measurement Location and Range

As noted by Scallion (ref. 5) and Siemers (ref. 6), the number of pressure orifices in the DFI is quite small, and considerable judgment must be exercised in the interpretation of the data. A review of the basic flow field phenomena associated with a complex vehicle such as the Space Shuttle orbiter, which incorporates both a reaction control system and aerodynamic control surfaces, indicates that the spatial distribution, limited number, and limited range of the measurements severely restrict analysis of the flight system. This conclusion has been confirmed by an inability to isolate specific flow phenomena such as control surface flow separation, RCS/control surface interaction, and the cause of lofting on ascent based on available flight data. An inability to resolve these problems from the flight data indicates that a substantially more elaborate measurement system would be required to isolate and define the flow field phenomena involved. Even though many of the flow field phenomena were predicted (allowing the proper location of pressure orifice and ranging of the transducers), some were not. Therefore, the measurement system must retain a flexibility which will allow the addition of new orifices, the relocation of others, and the change-out of transducers not on the proper operational range. In his study of Reaction Control System performance, Scallion (ref. 5) observed that "about half of the transducer pressure ranges were exceeded (the gages became saturated)." This gage saturation severely limited the thoroughness of the analysis. Because of

saturation, a limited DFI transducer change-out was accomplished at two locations in an attempt to better understand the pressure distributions relative to ascent lofting. Many times, however, the inclusion of a high-range transducer will result in an unacceptable decrease in data resolution at lower pressures. Under these circumstances, it would be necessary to incorporate dual transducers at these pressure ports. This design will provide the capability to obtain the data over the entire pressure range with good resolution. Such a dual system as incorporated in SEADS would have considerably enhanced much of the DFI data.

DFI FLIGHT DATA COMPARISONS

In spite of the shortcomings thus far described, useful results were obtained from the pressure data analyses performed. One objective of the evaluation of the STS-1-5 pressure data was to define flight pressure distributions for comparison with wind tunnel and computational data and to identify inconsistencies, if any. These comparisons contribute both to the validation of the orbiter's design and the demonstration of its flight worthiness, as well as provide a valuable data base for evaluating ground-based research capabilities. In addition, these comparisons determine the need for improvements in existing capabilities or requirements for new capabilities. Typical results from selected ports from STS-3 and -5 are shown in figures 12 through 16. Symbol identification is given in Table 1.

Data from the pressure port nearest the nose on the lower surface are shown in figures 12 and 13. This orifice has two transducers collocated at the same port with two different pressure ranges. The 0 to 15 psi transducer (V97P9100) data are shown in figure 12. Its data resolution for the 8-bit data system is 8.44 psf. For regions in the upper atmosphere, where pressure levels are low, the transducer output appears extremely noisy, but this is in actuality only a function of the resolution of the data system. Data below Mach 10 are much smoother. Both the wind tunnel and the HALIS data for this location match the flight data well, within the error band of the flight data. Where angle-of-attack excursions (aeromaneuvers) are noted in the flight pressure data, corresponding ground-based information gives similar nondimensional pressure levels. This can be noted in this and other figures for Mach 15 (HALIS) during STS-3.

The other transducer located at this same port has a 0 to 150 psf range (V37P9451). Its data resolution is 0.586 psf, and due to its location near the stagnation point and its shortened data range, the transducer is saturated shortly after the orbiter comes out of blackout. This transducer, with much better data resolution, gives a smoother set of flight data in the upper atmosphere, as evidenced in the STS-3 plot. The HALIS calculations matched well in the hypersonic region and predicted the correct pressure level at Mach 15 during the STS-3 aeromaneuver. In this and other plots, both the wind tunnel and HALIS data follow the shape of the flight data curves. For this transducer, however, the ground-based data are slightly higher than the flight data.

Figures 14 through 16 show comparisons of typical flight data with ground-based data. All of these DFI ports have 0 to 150 psf transducers which

provide good data resolution. All of the ground-based data are well within the flight data error band. Saturation of these transducers occurs around Mach 1.5 for each flight. This array of transducers is an excellent example of the calibration/bias uncertainties. The V07P9453 and V07P9461 transducers have unknown negative biases. For V07P9453, the flight data are consistently lower than the ground-based data for all three flights indicating that a bias correction could result in better agreement among data sources. The data obtained for V07P9461 are slightly higher than ground-based data. A bias correction would not help the agreement. This is an indication that the bias may be only slightly negative and may be a function of temperature. This slight disagreement could also be caused by the use of the "universal" calibration curve. The V07P9457 transducer has a positive bias which is subtracted from the flight data presented. Even though subtraction of the on-orbit bias lowered the flight data and provided good agreement with the ground-based data, the flight data are still slightly above ground-based results indicating possible temperature variation of the bias.

A review of the data presented in this paper and in references 1 and 2 reveals that, in spite of the many uncertainties in the flight data due to the limitation of the measurement/data system, the agreement is generally good between the flight and ground-based data. Generally, the ground-based data match the shape of the flight data, and observed biases are within the expected DFI measurement system error bands. Confidence in the data base could be improved with the incorporation of an improved measurement/data system.

AIR DATA PARAMETER EXTRACTION FROM DFI PRESSURES

Another objective, only partially attainable due to data limitations and the nonoptimal location of the DFI orifices for this purpose, was a test of the capability of the SEADS method to extract typical air data from DFI pressures. The method used for this purpose is an adaptation of the SEADS flight data computational technique described in detail in references 6 and 8. The basic SEADS technique derives vehicle attitude and free-stream dynamic pressure from the nose region pressure distribution.

For Shuttle orbiter flights STS-1-5, DFI pressure measurements were available at the ports shown in figures 1-3. Only three orifices were considered far enough forward to furnish reliable data representable by the SEADS pressure model. Some of the farther aft orifices on the bottom of the fuselage were considered and were determined to degrade the analysis accuracy. The data from the top orifice was suspect due to possible flow separation at high angles of attack (α), and then the transducer saturated at lower angles (and altitudes), furnishing no useful pressure data for this study. This analysis has thus been restricted to the front fuselage orifices located on the bottom, (P_b), and port side, (P_p). Since no orifice was located on the forward starboard side, the sideslip angle (β) was not obtained. The two pressures, P_b and P_p , permit the solution for only two state variables: angle of attack (α) and free-stream dynamic pressure (q_∞). These physical limitations of the DFI result in the introduction of two simplifying assumptions, neglecting sideslip angle and ambient pressure.

Again, since the DFI recorder did not operate during the STS-1 and STS-4 missions and the complete DFI system was not activated during STS-2, only STS-3 and STS-5 have provided complete sets of data for this part of the study.

The first try (using no external data sources) at obtaining α and q_{∞} is shown in figures 17 and 18. This analysis was terminated at approximately $M = 3$, where the low-range transducer P_b saturates. It is seen that the trend of trajectory determined α (labeled BET) was followed well with an error of approximately 2° to 3° . The importance of a high-resolution data system is also obvious in the flight data as the data scatter increases greatly below $M = 10$ where P_b makes a transition from the 0-1 psi to the 0-15 psi transducer.

Because of the limitations imposed by lack of pressure orifices in the nose region, the angle of attack derived from using the SEADS algorithm with the DFI pressures may be questioned when compared to α derived from trajectory or navigation data. Nevertheless, the trends in α are modeled well, and the dynamic pressure is predicted quite accurately. Analysis indicates that distinct improvements in this SEADS method will result when pressure distributions on the nose cap are available.

Comparisons of the final SEADS/DFI derived q_{∞} from STS-3 and STS-5 with other sources of q_{∞} show that in the hypersonic flight regime the SEADS/DFI - q_{∞} agrees with the G & C - q but differs from the Best Estimate Trajectory (BET)- q_{∞} by a small, though percentagewise, significant amount. Additional analysis by LaRC (refs. 9, 10), JSC, and Rockwell International has shown that the BET- q_{∞} in this region leads to values of the aerodynamic coefficients at variance with their predicted values. While resolution of this discrepancy must await a Shuttle orbiter flight with SEADS onboard, the SEADS/DFI derived value has been accepted as representative in the hypersonic region and has been included in the LaRC BET in this region for STS-3 and -5.

RECOMMENDATIONS

Although significant results have thus far been obtained as a result of the analyses conducted using the DFI pressure data from STS-1 through STS-5, these results are severely limited because of the limitations which have been shown to exist in the DFI. Design of future pressure measurement systems for flight system performance evaluations should incorporate the following improvements.

1. Design the data system to provide the data accuracy, resolution, and frequency required to evaluate the flow field phenomena of interest as well as accepting the bias or other idiosyncrasies of the measurement system.
2. Proper selection of number and location of measurements is dependent on available ground data base.
3. Proper ranging of transducers based on predicted pressure-field analysis and available ground data base is necessary.

4. Measurement system should be of a design to allow changes resulting from preflight end-to-end system tests as well as initial flight tests to improve the quantity or quality of the data.
5. Component temperature monitoring and calibration based on nominal temperature profiles are required. Since the response to temperature variation is highly nonlinear, calibration should be performed throughout the expected temperature range.
6. Individual calibration curves of all transducers in the system should be used. "Family" calibrations are not adequate.
7. Transducer biases, both positive and negative, should be accommodated in the data system.
8. In situ reference values (for example, on-orbit pressure zeros, supply voltage, and temperature) should be used in data reduction.

SUMMARY AND CONCLUSIONS

Pressure data obtained from the Space Shuttle orbiter's Development Flight Instrumentation in the forward fuselage region during the STS-1 through -5 reentries have been compared to wind tunnel and computational data. Ground-based data across the speed range matched the flight data within the uncertainty calculated for the DFI system. An analysis of the DFI data system and the calibration procedures associated with the in-flight behavior of the transducers has provided a better understanding of the DFI system and explained differences between the ground-based data and the flight data.

As a result of the analyses presented, certain conclusions are noted here. Agreement between ground-based and flight data, although good, is limited by the resolution of the flight data system and the preflight calibration of the transducers. Improved data system resolution and more thorough transducer calibration could reduce the uncertainty from 5 percent to 0.1 percent full scale. More pressure measurements and transducers of different ranges (more applicable to the reentry environment) are needed onboard the orbiter for accurate pressure modeling. Orifice leakage and tile steps and gaps are not important to the response and accuracy of the DFI flight pressure data given the resolution and quality of the system. Both the wind tunnel tests completed on the forward fuselage models and the HALIS computer program predict in-flight forward fuselage pressure distributions well. Both ground-based techniques can be used confidently, although HALIS data are currently restricted to the windward surface. The technique developed for SEADS to derive accurate air data parameters from forward fuselage pressures has been demonstrated with the DFI data.

REFERENCES

1. Siemers, P. M., III: Shuttle Entry Air Data System. Paper presented at the 1978 Air Data Systems Conference, Colorado Springs, Colorado, May 3, 1978.
2. Bradley, P. F., Siemers, P. M., III, and Pruett, C. D.: Comparison of Forward Fuselage Space Shuttle Orbiter Flight Pressure Data to Wind-Tunnel and Analytical Results in the Hypersonic Mach Number Range. AIAA Paper 81-2477, November 1981.
3. Weilmuenster, K. James, and Hamilton, H. Harris II: A Method for Computation of Inviscid Three-Dimensional Flow Over Blunt Bodies Having Large Embedded Subsonic Regions. AIAA Paper 81-1203, June 1981.
4. Bradley, P. F., Siemers, P. M., III, and Weilmuenster, K. J.: An Evaluation of Space Shuttle Orbiter Forward Fuselage Surface Pressures: Comparison With Wind Tunnel and Theoretical Predictions. AIAA Paper 83-0119, January 1983.
5. Scallion, W. I., Compton, H. R., Suit, W. T., Powell, R. W., Blackstock, T. A., and Eates, B. L.: Space Shuttle Third Flight (STS-3) Entry RCS Analysis. AIAA Paper 83-0116, January 1983.
6. Siemers, P. M., III, Wolf, H., and Flanagan, P. F.: Shuttle Entry Air Data System Concepts Applied to Space Shuttle Orbiter Flight Pressure Data to Determine Air Data STS 1-4. AIAA Paper 83-0018, January 1983.
7. Stoddard, L. W., and Draper, H. L.: Development and Testing of Development Flight Instrumentation for the Space Shuttle Thermal Protection System. Proceedings of the 24th International Instrumentation Symposium, Part 2, Instrumentation Society of America, 1978, pp. 663-672.
8. Pruett, C. D., Wolf, E., Siemers, P. M., III, and Heck, M. L.: An Innovative Air Data System for the Space Shuttle Orbiter: Data Analysis Technique. AIAA Paper 81-2455, November 1981.
9. Compton, H. R., Scallion, W. I., Suit, W. T., and Schiess, J. R.: Shuttle Entry Performance and Stability and Control Derivative Extraction From Flight Measurement Data. AIAA Paper 82-1317, August 1982.
10. Findlay, J. T., and Compton, H. R.: On the Flight Derived/Aerodynamic Data Base Performance Comparisons for the NASA Space Shuttle Entries During the Hypersonic Regime. AIAA Paper 83-0115, January 1983.

TABLE 1

SYMBOL IDENTIFICATION FOR DATA PLOTS

— FLIGHT DATA

HALIS

WIND TUNNEL

- ▶ Mach 20.
- ⊙ Mach 18.
- ▲ Mach 15.3
- Mach 10.

- Mach 10.
- Mach 6.
- ◇ Mach 4.63
- △ Mach 3.5
- ▵ Mach 2.96
- ▷ Mach 2.3
- ◻ Mach 2.
- ◊ Mach 1.5

ORIGINAL PAGE IS
OF POOR QUALITY

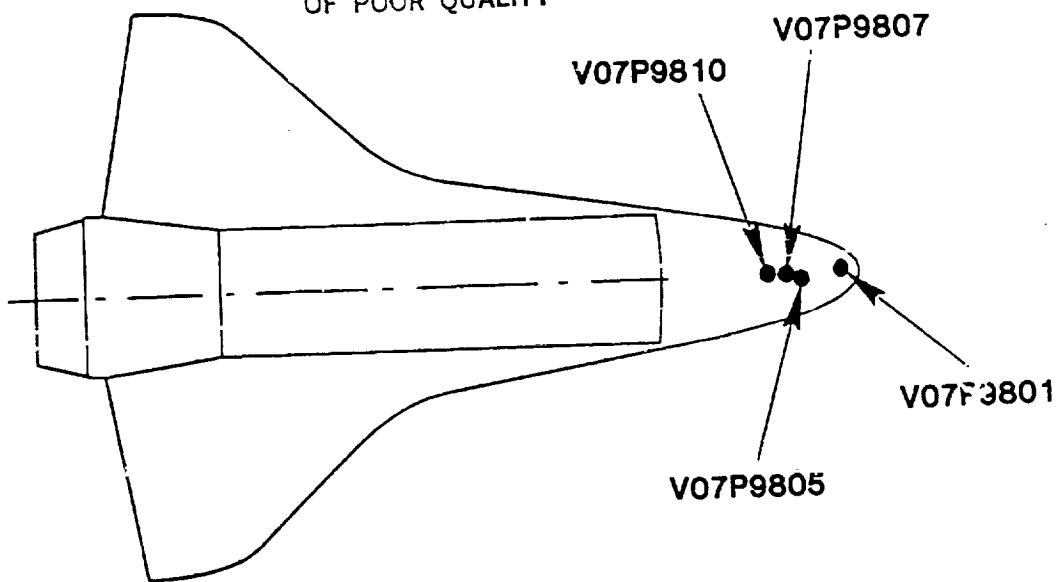


Figure 1.- Upper surface DFI pressures.

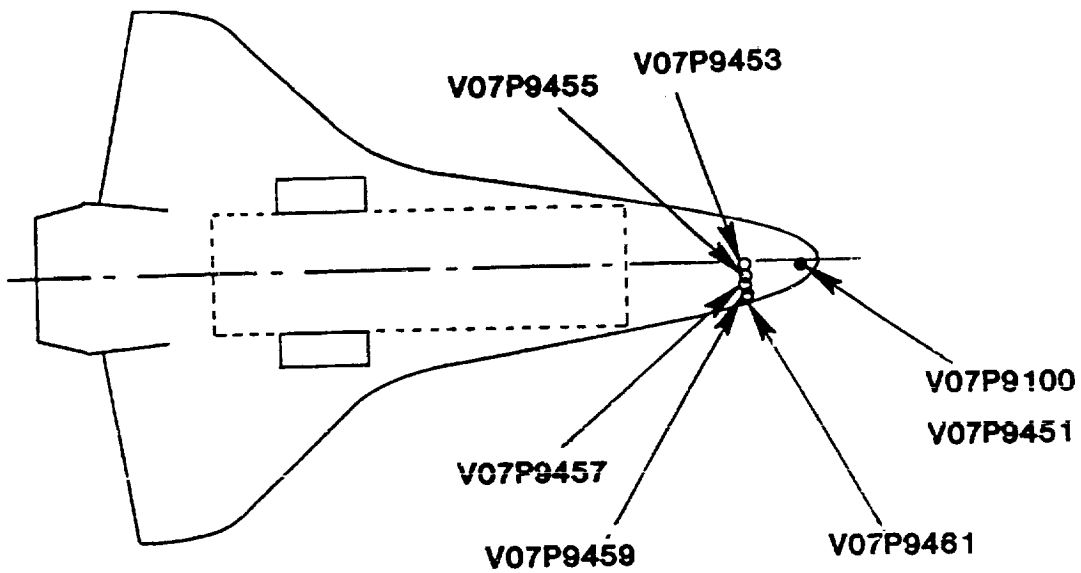


Figure 2.- Lower surface DFI pressures.

ORIGINAL PAGE IS
OF POOR QUALITY

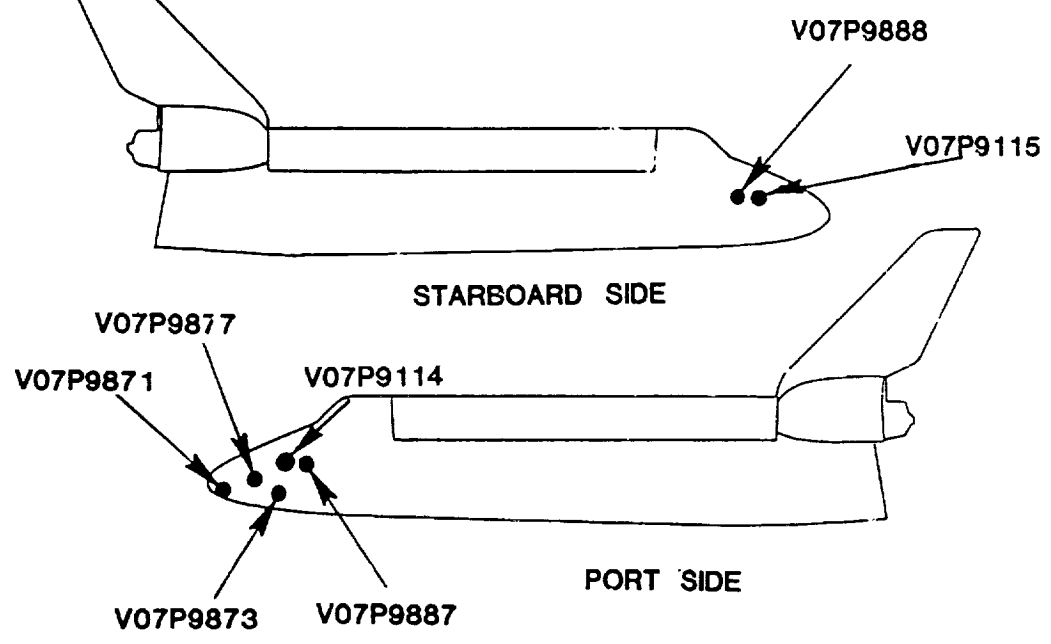


Figure 3.- Port and starboard DFI pressures.

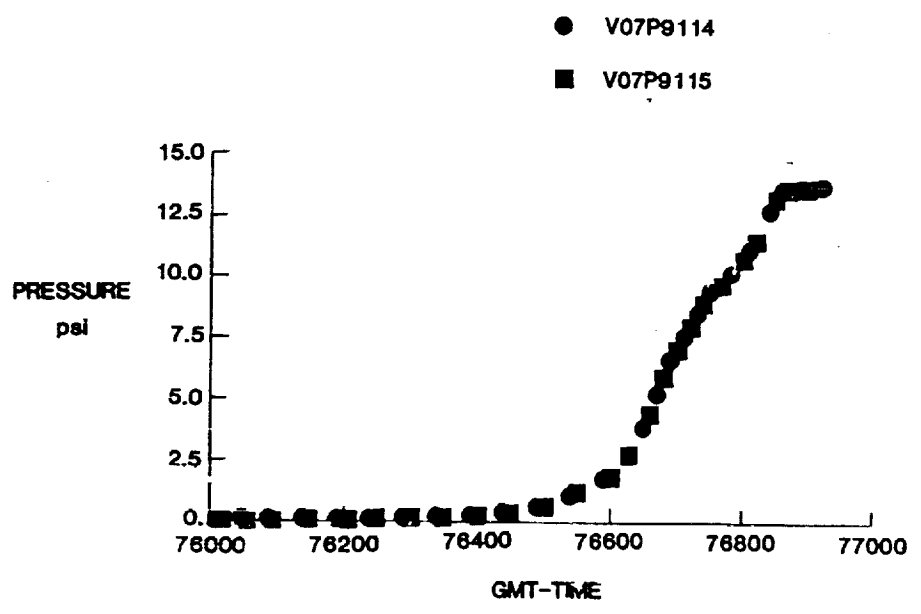


Figure 4.- STS-2 pressure data for V07P9114 and V07P9115.

ORIGINAL PAGE IS
OF POOR QUALITY

WIND TUNNEL DATA ●

FLIGHT DATA —

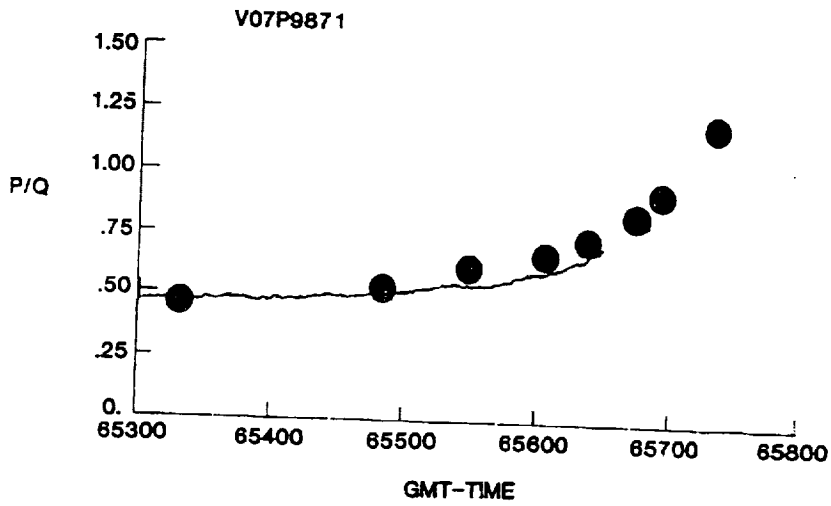


Figure 5.- STS-1 pressure data for V07P9871 compared to wind tunnel results.

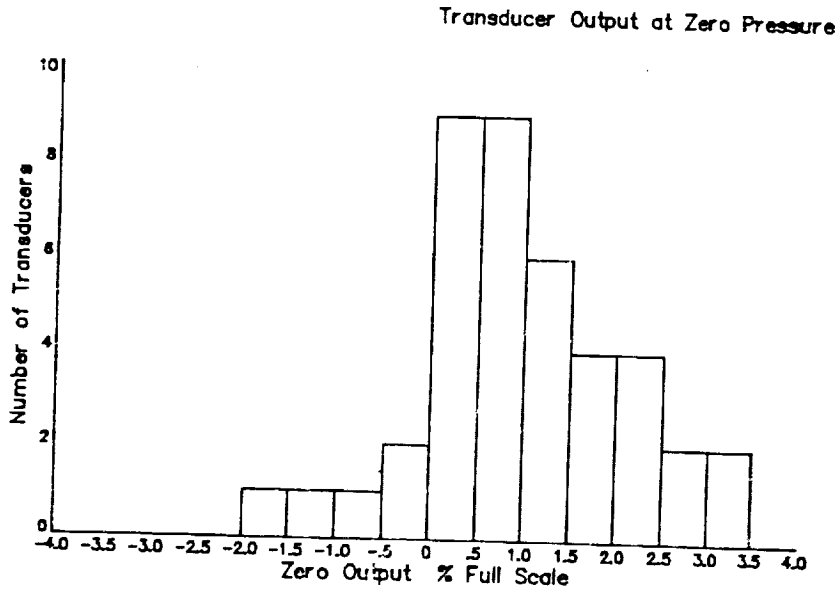


Figure 6.- Zero balance distribution (41 transducers).

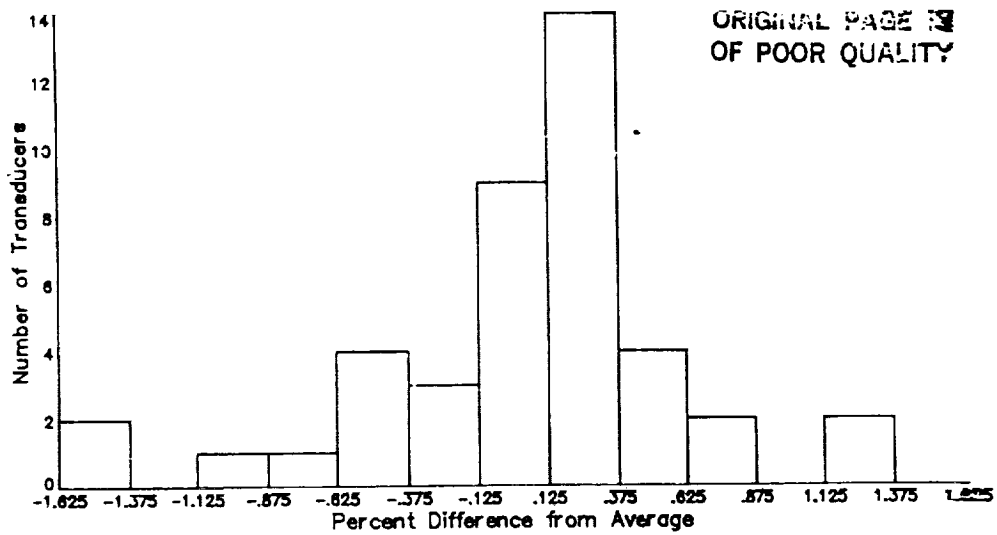


Figure 7.- Sensitivity distribution (42 transducers).

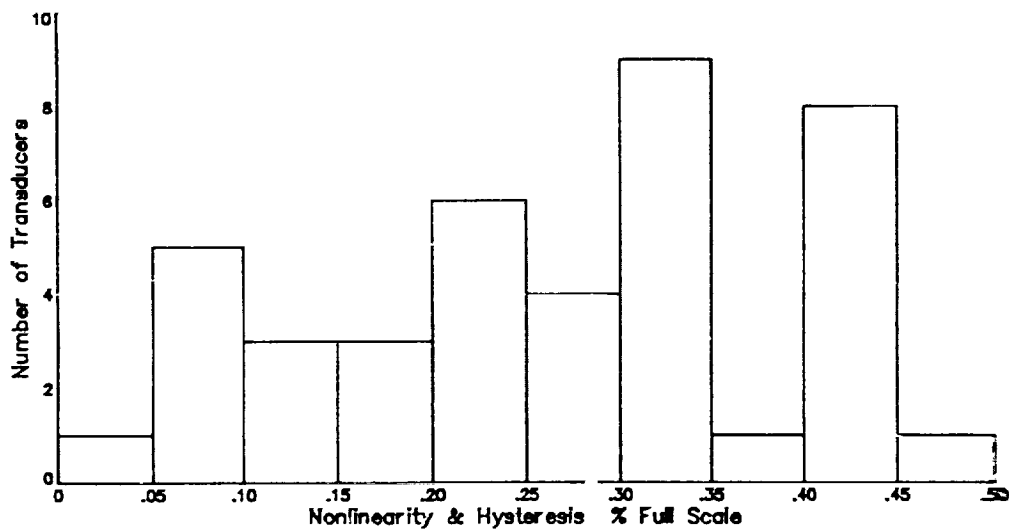


Figure 8.- Nonlinearity and hysteresis distribution (41 transducers).

Temperature Range -79° to 113° C

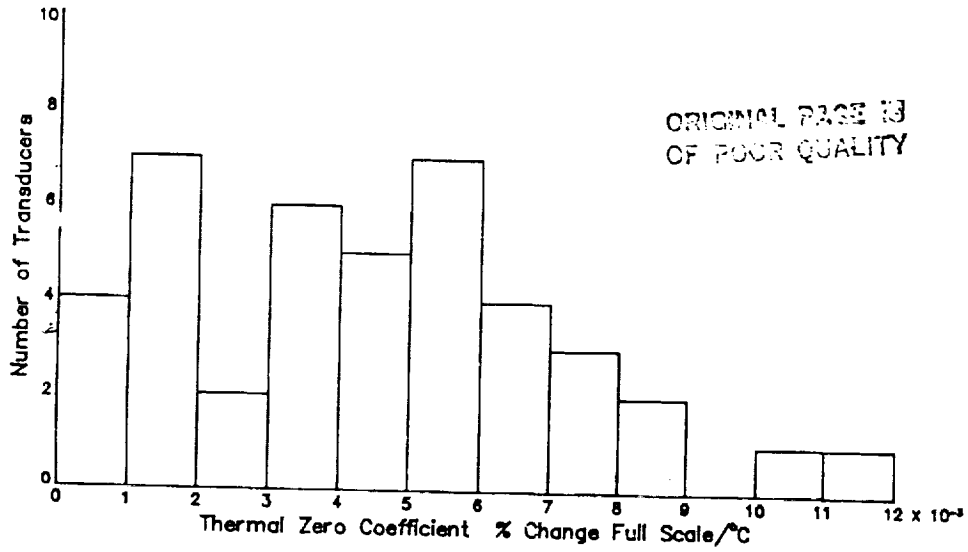


Figure 9.- Thermal zero-coefficient distribution (42 transducers).

Temperature Range -79° to 113° C

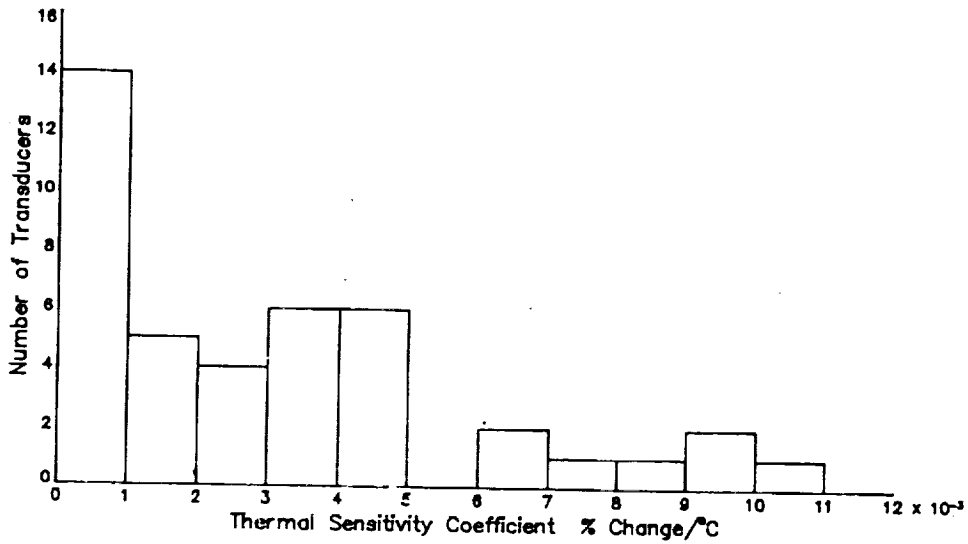


Figure 10.- Thermal sensitivity coefficient distribution (42 transducers).

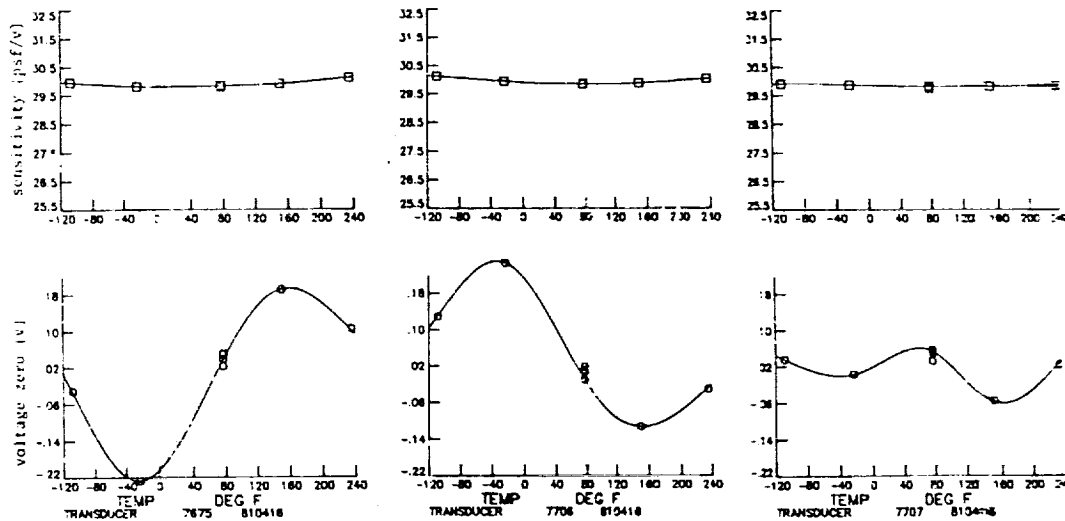


Figure 11.- Typical transducer temperature variations.
(See table 1.)

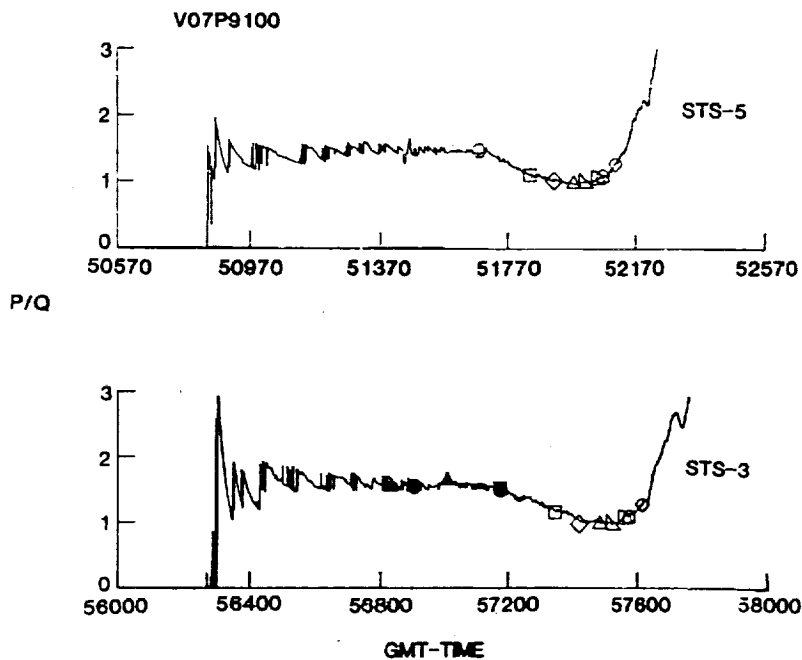


Figure 12.- STS-3 and STS-5 pressure data for V07P9100 compared to ground-based results. (See table 1.)

ORIGINAL PAGE IS
OF POOR QUALITY

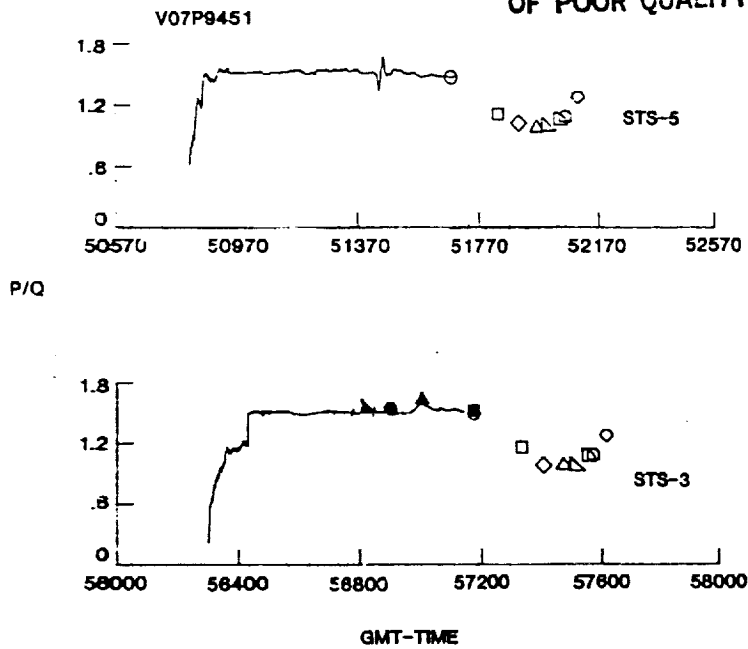


Figure 13.- STS-3 and STS-5 pressure data for V07P9451 compared to ground-based results. (See table 1.)

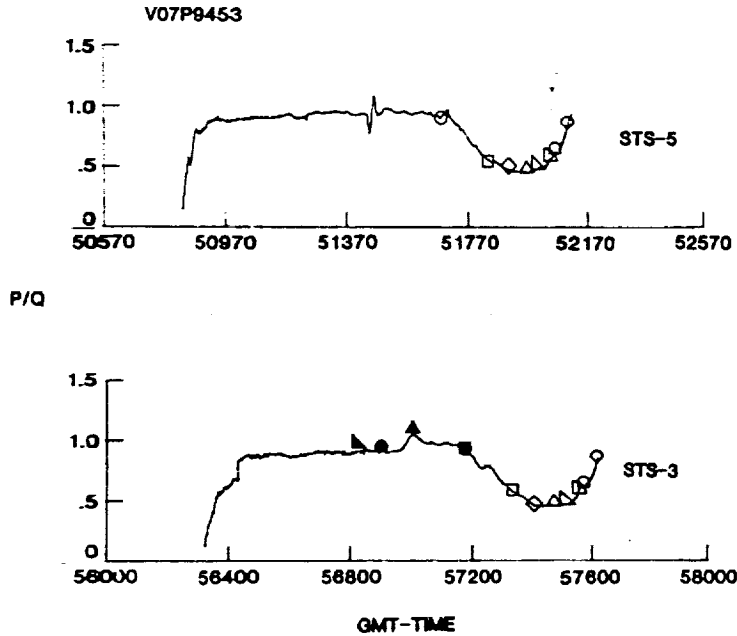
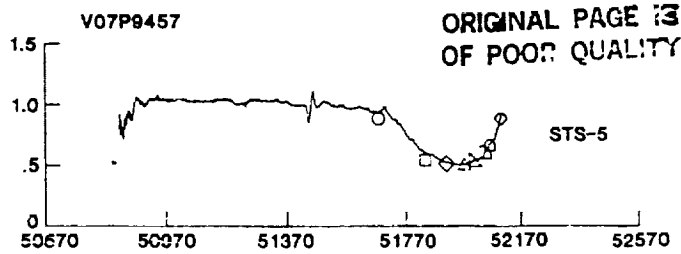


Figure 14.- STS-3 and STS-5 pressure data for V07P9453 compared to ground-based results. (See table 1.)



P/Q

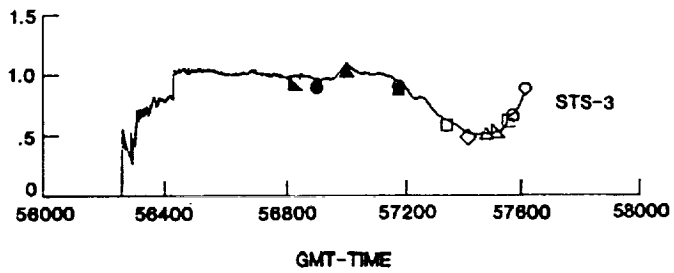
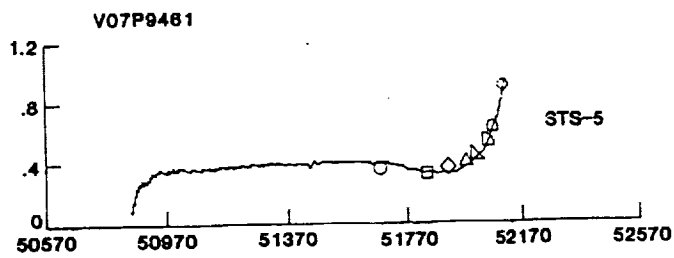


Figure 15.- STS-3 and STS-5 pressure data for V07P9457 compared to ground-based results. (See table 1.)



P/Q

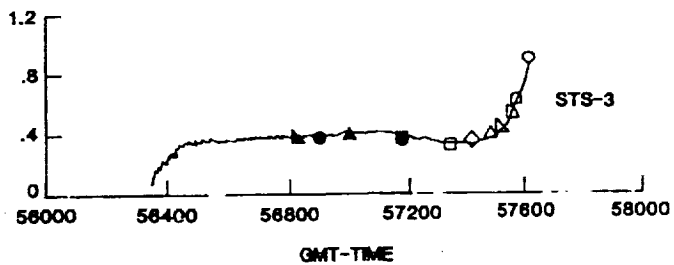


Figure 16.- STS-3 and STS-5 pressure data for V07P9461 compared to ground-based results. (See table 1.)

ORIGINAL PAGE 13
OF PGOR QUALITY

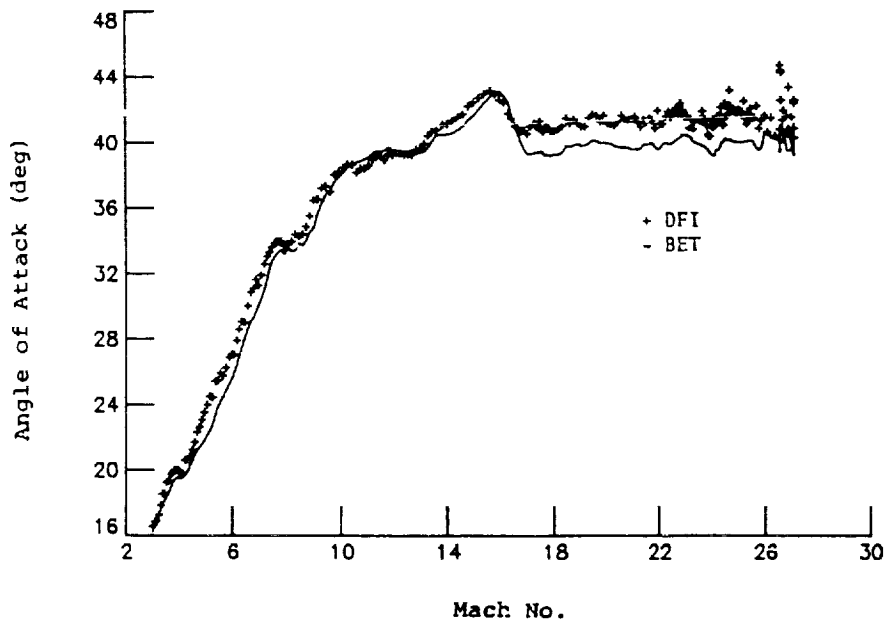


Figure 17.- STS-3 DFI/SEADS derived angle of attack.

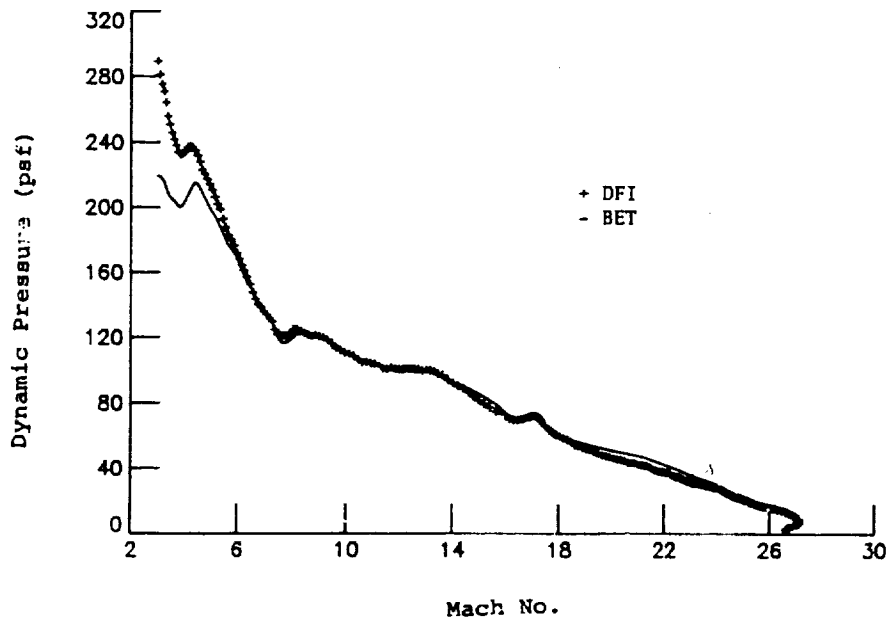


Figure 18.- STS-3 DFI/SEADS derived dynamic pressure.